ARTICLE

OBC
www.rsc.org/obc

Effects of an 8-bromodeoxyguanosine incorporation on the parallel quadruplex structure $[d(TGGGT)]_4$

Veronica Esposito,[a] Antonio Randazzo,[a] Gennaro Piccialli,[a] Luigi Petraccone,[b] Concetta Giancola[b] and Luciano Mayol*[a]

[a] *Dipartimento di Chimica delle Sostanze Naturali, Università degli Studi di Napoli "Federico II", via D. Montesano 49, I-80131 Napoli, Italy. E-mail: mayoll@unina.it; Fax: +39-081-678552; Tel: +39-081-678508*

[b] *Dipartimento di Chimica, Università degli Studi di Napoli "Federico II", via Cintia, I-80126, Napoli, Italy*

Received 14th November 2003, Accepted 10th December 2003
First published as an Advance Article on the web 12th January 2004

NMR, molecular dynamics and mechanics calculations, and CD spectroscopy were used to characterise three tetramolecular quadruplex complexes: $[d(TG^{Br}GGT)]_4$, $[d(TGG^{Br}GT)]_4$ and $[d(TGGG^{Br}T)]_4$, where G^{Br} indicates an 8-bromoguanine residue. All three quadruplexes are characterised by a 4-fold symmetry with all strands parallel to each other and, differently to what has been observed for other parallel quadruplex structures, with a tetrad (formed by 8-Br-dGs) in a *syn* conformation. The whole of the data demonstrates that the replacement in turn of different dG residues with 8-Br-dG in the sequence 5′-TGGGT-3′ affects the resulting structures in different ways, leading to different CD profiles and thermal stabilities. Particularly, $[d(TG^{Br}GGT)]_4$ and $[d(TGG^{Br}GT)]_4$ are more stable than the unmodified sequence, whereas $[d(TGGG^{Br}T)]_4$ is much less stable than the natural counterpart. The conformational features found in the three quadruplexes might, in principle, amplify the range of applicability of synthetic oligonucleotides as aptamers or catalysts, by providing novel structural motifs with different molecular recognition capabilities from those of native DNA sequences.

Introduction

Noncoding repeat sequences of guanine-rich DNA are particularly important at the ends of chromosomes, where they form protein-DNA assemblies, well-known as telomeres. Telomeric DNA contains runs of guanine bases that can adopt an important structural motif based on G-quartets, cyclic hydrogen-bonded arrays of four coplanar guanine bases, stacking on top of each other to form G-quadruplexes. Guanosine-rich clusters can fold in a number of different ways, as far as strand stoichiometry and orientation are concerned. Strand stoichiometry variation allows G-quadruplexes to be formed by association of one, *via* intramolecular folding,[1–3] two, by dimerization of a folded-back hairpin,[4–5] or four separate strands.[6–7] It has been demonstrated by footprinting, strand mixing and cross-linking studies,[8–10] along with NMR spectroscopy and X-ray crystallography[6,11] that single dG_n segments can form a tetramolecular complex with all G bases in the *anti* conformation and all strands parallel to each other in monovalent cation containing solution, while the folded-back dimeric quadruplex has alternating *syn* and *anti* nucleotide conformations along each strand and two pairs of adjacent parallel strands.[4–5,12–13] Furthermore, oligonucleotides, forming a unimolecular quadruplex, as the thrombin-binding DNA aptamer (TBA) for an example, show the residues of the tetrads in an *anti-syn-anti-syn* conformation with alternating antiparallel strands.[12,14–15]

In addition to their presence at the telomeric ends of eukaryotic chromosomes,[16–17] runs of dGs may also be involved in recombination and mutation hot spot processes,[18–22] gene regulation[23] and various human diseases.[24–25]

Considering that a wider biological relevance for quadruplex DNA is now becoming apparent and that the G-tetrad repeating motif tolerates a surprisingly broad range of structural features, it may be interesting to investigate the changes in structure and activity that occur upon structural modification. In order to explore this case, we report here a structural study, based on NMR and CD spectroscopy, and molecular mechanics and dynamics calculations, of the quadruplexes $[d(TG^{Br}GGT)]_4$, $[d(TGG^{Br}GT)]_4$ and $[d(TGGG^{Br}T)]_4$, where G^{Br} indicates an 8-bromoguanine residue, which was incorporated at different positions in the sequence. The substitution of a single atom in guanine may indeed produce remarkable changes in the physical and biological properties of the resulting nucleic acid fragments. Bromination of a guanosine residue is of particular interest for many reasons. As a matter of fact, the immunological and biological relevance of the 8-bromoguanosine 3′,5′-cyclic monophosphate has been already reported.[26] Furthermore, the investigation of brominated oligonucleotides are of interest for electron transfer studies within DNA molecules, due to the potential of 8-Br-dG residues to act as a sink for electrons.[27] In addition, this modified base was used to reduce the conformational heterogeneity of RNA[28] and to probe the conformation about glycosidic bonds in unusual nucleic acid structures.[29] In fact, the presence of a bulky substituent such as the bromine atom at the C8 position of guanosine destabilizes the normal *anti* orientation of the base, sterically constraining the glycosidic bond to the *syn* conformation.[30] This implication was already investigated for a unimolecular antiparallel stranded quadruplex, of sequence 5′-d(TTTGGTTTGGTTTGGTTT-GG)-3′, in which the substitution of an 8-Br-dG at positions with *syn* conformations in G-quartet arrangements stabilizes the structure, while the substitution at positions required to be *anti* destabilizes the quadruplex.[29] In this paper we describe the effects of this brominated base on a tetramolecular parallel stranded quadruplex structure $[d(TGGGT)]_4$, that usually shows all bases of tetrads in a glycosidic *anti* conformation.

Results and discussion

The pentanucleotide 5′-d(TGGGT)-3′, in the presence of potassium ions, forms a stable tetramolecular helix, already characterised by thermodynamic and spectroscopic techniques,[31] with all strands parallel to each other and all guanines in *anti* glycosidic conformations. In order to test the effects of the incorporation of 8-bromodeoxyguanosine (8-Br-dG) on the

DOI: 10.1039/b314672c

Table 1 Non-exchangeable proton chemical shifts (500 MHz) for **M1**, **M2**, and **M3** quadruplexes in 10 mM KH_2PO_4, 70 mM KCl, 0.2 mM EDTA (pH 7.0, T = 300 K)

	Base (5′–3′)	H8/H6	H1′	H2′/H2″	H3′	H4′	H5′/H5″	H2/Me
M1	T	7.45	6.11	2.22–2.54	4.78	4.13	3.58–4.04	1.58
	G^{Br}		6.10	3.02–3.91	5.02	4.39	4.24	
	G	8.15	5.78	2.67	5.08	4.42	4.33	
	G	7.72	6.28	2.51–2.67	4.91	4.52	4.27	
	T	7.36	6.08	2.16	4.47	4.47	4.07–4.23	1.64
M2	T	7.37	5.93	2.10–2.26	4.68	4.68	4.04	1.42
	G	8.15	6.27	2.91–3.4	5.03	4.42	3.90–4.04	
	G^{Br}		6.16	2.93	5.12	4.45	4.19	
	G	7.88	6.21	2.51–2.66	5.02	4.46	4.26	
	T	7.32	6.07	2.14	4.48	4.48	4.06–4.24	1.69
M3	T	7.52	5.96	2.19–2.51	4.75	4.13	3.79	1.43
	G	8.16	6.11	2.74–2.94	5.06	4.45	4.16–4.28	
	G	7.58	6.36	2.61–2.88	5.07	4.53	4.14–4.28	
	G^{Br}		6.24	2.59–3.44	5.03	4.53	4.06–4.20	
	T	7.33	6.02	2.17	4.53		4.01	1.61

thermal stability and structure of this quadruplex we replaced all the canonical dG residues, one by one, with the brominated nucleoside. Commercially available 5′-DMT-aminoprotected-8-bromodeoxyguanosine-3′-phosphoramidite was used for the preparation of the modified oligonucleotides. Hence the pentamers 5′-d(TG^{Br}GGT)-3′ (**M1**), 5′-d(TGG^{Br}GT)-3′ (**M2**), and 5′-d(TGGG^{Br}T)-3′ (**M3**), were assembled using standard solid phase β-cyanoethylphosphoramidite chemistry. The crude oligomers were purified by HPLC and desalted. The NMR samples were prepared at a concentration of 1.0 mM (0.5 ml, 90% H_2O/10% D_2O), with 10 mM potassium phosphate, 70 mM KCl, 0.2 mM EDTA (pH 7.0) buffer. The samples were annealed for 5–10 minutes at 80 °C and slowly cooled down to room temperature, then their ^{1}H-NMR spectra were recorded by using pulsed-field gradient WATERGATE[32] for H_2O suppression. Concerning **M1** and **M2**, the ^{1}H-NMR spectra (500 MHz, T = 300 K) show the presence of three well defined singlets in the region 11–12 ppm, attributable to imino protons involved in Hoogsteen hydrogen bonds of G quartets, and of four signals, belonging to two guanine H8 and two thymine H6 protons in the aromatic region. This indicates, in both cases, the presence in solution of a single well defined quadruplex species, consisting of three G-tetrads and possessing a 4-fold symmetry with all strands parallel to each other. On the other hand, the spectrum of **M3** at the same temperature shows the presence of eight signals in the range between 7.2 and 8.2 ppm, and only three imino peaks in the region 11–12 ppm. Raising the temperature to 325 K, four out of the eight signals gradually increased in intensity, whereas the other four, along with the three imino peaks, disappeared progressively. Thus, at 325 K only four signals were present in the aromatic region of the ^{1}H-NMR spectrum, while no imino peak was present. This suggested that at 325 K **M3** exists exclusively as a single strand, while at 300 K the quadruplex structure is in equilibrium with its single strand, that represents the prevalent species at this temperature. Unfortunately, the quadruplex/single strand ratio could not be increased by diminishing the temperature to 283 K. The quadruplex structure formed by **M3**, as well as the ones formed by **M1** and **M2**, are parallel stranded with a 4-fold symmetry, as suggested by the number of imino peaks.

The exchange rates of the imino protons of **M1**, **M2** and **M3** with solvent were qualitatively estimated by partially drying the samples in water and reconstituting them in D_2O. Periodic examination of the imino proton signals shows that they are significantly inaccessible to the solvent, in agreement with observations on other quadruplex structures.[33]

Proton signals for **M1**, **M2** and **M3** have been almost completely assigned on the basis of NOESY and TOCSY data obtained at 500 MHz (T = 300 K), as shown in Table 1. As reported for other parallel quadruplex structures,[34–35] the polarity connectivities (G H8 to ribose protons on the 5′ side only) suggested the right handed nature of the helices of the quadruplexes. As for the glycosidic torsion angles of the G residues, useful information could be obtained analysing the relative intensities of NOEs between G H8 and ribose H2′ compared with the NOEs observed between G H8 and H1′. Thus, as for unmodified G residues, weak NOEs between G H8 and H1′ and strong NOEs between G H8 and ribose H2′ indicate that all unmodified G residues are in an *anti* conformation. Unfortunately, the lack of the H8 proton in the 8-Br-dG residues prevented us from determining the conformation of the glycosidic torsion angle for these residues.

2D NOESY spectra (mixing time = 100 ms) were used to extract distance constraints in order to determine the three-dimensional structures of quadruplex structures formed by **M1**, **M2** and **M3**. The Overhauser effect intensities were converted into distances by the CALIBA tool of the CYANA program.[36] Pseudo-atoms were introduced where needed for all three structures.

Structure determination of M1

As concerning the quadruplex structure adopted by **M1**, 256 upper distance restraints were calculated and reduced to 112 after removal of irrelevant restraints. Backbone torsion angles were restricted to be in a range of ±20° of helical values of the natural quadruplex [d(TGGGT)]$_4$, except for the 8-Br-dG residue, in fact for this a range of ±40° was used in order to allow it a wider conformational flexibility. Glycosidic torsion angles for all unmodified guanines were kept in a range of −157° to −97° (*anti* conformation), whereas for 8-Br-dG residues, where the bulky substitution at the C8 position constrains the glycosidic bond to the *syn* conformation,[30] a range of −10° to 90° was used. In order to rule out the possibility that the 8-Br-dGs adopt an *anti* conformation, molecular models for each sample, **M1**, **M2** and **M3** were built, where the *chi* angle was imposed in the *anti* conformation. In all three cases, the models showed heavy distortions of the backbone in reason of the unfavourable steric interactions between the bromine and the deoxyribose unit. Furthermore, according to an NH deuterium exchange study, three layers of G-tetrads were built using 48 supplementary distance restraints (HN1–O6, N1–O6, HN2–N7, N2–N7) for 24 hydrogen bonds. As for the 8-Br-dG quartets, H-bonds were set according to the *syn* conformation of the glycosidic angles. The quadruplex structures were calculated by using the CYANA program.[36] The calculation started with 300 randomised conformers. The analysis was focalised on the 10 structures with the lowest CYANA target functions resulting from van der Waals and restraints violations. Thus, these structures were subjected to restrained energy minimization (no angle constraints were used) using the CVFF forcefield as implemented in the DISCOVER program (Molecular Simu-

lations, San Diego, CA, USA). Particularly, average RMSD values of 2.03 ±0.49 and 2.09 ±0.48 for the backbone and all heavy atoms, respectively, were obtained from their superimposition, suggesting that the structure adopted by **M1** is consistent with experimentally determined restraints. As expected, all the structures obtained reflect the right handed nature of the quadruplex helices with a 4-fold symmetry and all purine residues able to form tetrads, whereas the main differences are noteworthy at the modified residue level of the molecule. In fact all the minimised structures of **M1** show that the glycosidic torsion angles of the 8-Br-dG residues are in the range of 123°/173°, deviating from the canonical *chi* values of the *syn* range. However, all 8-Br-dG residues assume a planar arrangement and form Hoogsteen N1–O6 and N2–N7 hydrogen bonds. Furthermore, differently from that observed in the unmodified quadruplex $[d(TGGGT)]_4$, the five-membered rings of 8-Br-dG bases in $[d(TG^{Br}GGT)]_4$ stack completely over the five-membered rings of the underneath guanines (Fig. 1).

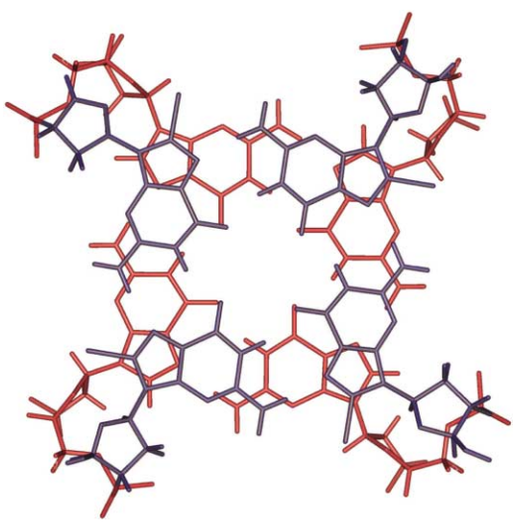

Fig. 1 Top view of the stacking observed between the five-membered rings of 8-Br-dG bases (in blue) and the five-membered rings of the underneath guanines (in red) in the mean structure of the **M1** quadruplex.

Structure determination of M2

As for **M1**, the CYANA program[36] was used to calculate the quadruplex structures of **M2**, starting with 300 randomised conformers and 252 upper distance restraints reduced to 100 after removal of the irrelevant restraints. 48 supplementary distance restraints (HN1–O6, N1–O6, HN2–N7, N2–N7) were introduced for 24 hydrogen bonds of the three G-quartets, whose presence was deducible from an NH deuterium exchange study. A range of ±20° around the canonical helical values of the natural quadruplex was fixed for the backbone torsion angles of the structure built for **M2**, but, whereas for all unmodified guanines the *chi* angle was kept in a range of −157° to −97° (*anti* conformation), for the 8-Br-dG residue a range of −10° to 90° (*syn* conformation) was used. The 10 best structures with the lowest CYANA target functions were energy minimized (without angle constraints) using the CVFF forcefield (see above) and then superimposed, obtaining average RMSD values of 2.10 ± 0.46 and 2.12 ± 0.46 for the backbone and all heavy atoms, respectively. As in the preceding case, the resulting structures showed a right-handed helicity and the guanine residues to have an almost planar conformation with three well-defined G-tetrads. Otherwise, the main differences could be noted at the central 8-Br-dG substitution level in comparison to that observed for **M1**. As a matter of fact, the C8–Br bonds of the modified guanines at the central positions resulted slightly distorted for the presence of steric effects between bromines and the 5′-phosphate groups of guanosine of the adjacent strand (Fig. 2). Differently from the preceding case, the five-membered rings of 8-Br-dG bases stack only partially over the five-membered rings of the underneath guanines (Fig. 3). Moreover, the six-membered rings of 8-Br-dG residues stack partially over the six-membered rings of the upper guanines (Fig. 3) and the glycosidic torsion angles of the modified bases fall perfectly in the *syn* range (7.3°–24.0°). It is interesting to note that four additional H-bonds between the hydrogens on the N2 (H22 or H21) of the 8-Br-dG residue and an oxygen of the phosphate group (OP2) of the same residue could be formed, at least in principle, in the quadruplex structures determined for **M2**.

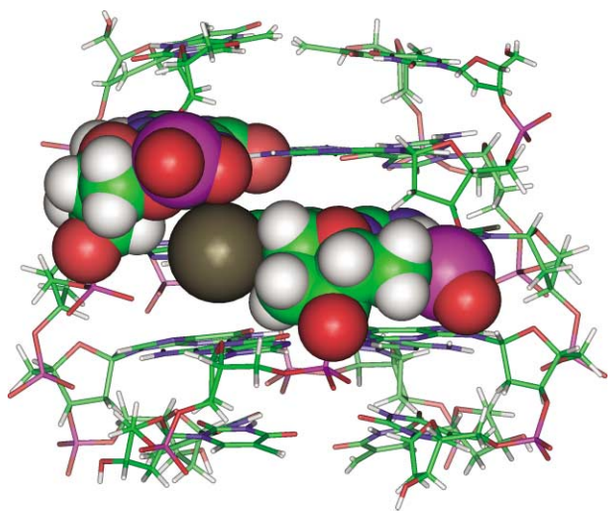

Fig. 2 Side view of average structure of the best 10 structures of the **M2** quadruplex. Heavy atoms are shown with different colors (carbons, green; nitrogens, blue; oxygens, red; hydrogens, white; bromine, dark brown); One 8-Br-dG residue and the dG residue of the adjacent strand are reported in CPK. The steric effect between bromine and the 5′-phosphate group of the guanosine of the adjacent strand is plainly observable.

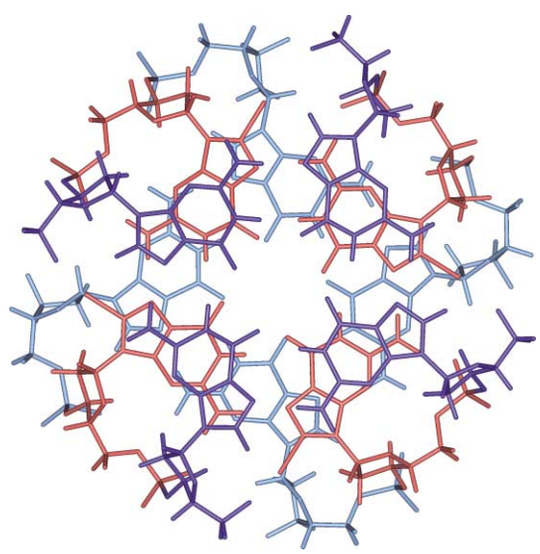

Fig. 3 Top view of the stacking observed between the 8-Br-dG tetrad (in red) and the adjacent dG-tetrads (in dark and light blue at the 5′ and 3′ sides respectively) in the mean structure of the **M2** quadruplex.

Structure determination of M3

As mentioned before, the quadruplex structure obtained by **M3** is in equilibrium with its single strand, which represents the prevalent species at 300 K. In spite of this, it was possible to study its three-dimensional structure since the NOESY spectra contain prevalently NOEs belonging to the structured molecule. The structural study of **M3** was, once more, performed by

using the CYANA program, starting with 300 randomised conformers. 144 distance restraints were effectively used for calculation, since 196 of the initial 340 were irrelevant. Hoogsteen N1–O6 and N2–N7 hydrogen bond restraints between guanine bases of the three G-tetrads, intelligible from NH deuterium exchange study, were additionally introduced. The backbone torsion angles for all canonical residues were kept in a range of ±20° around the helical values of the unmodified quadruplex $[d(TGGGT)]_4$. Further, the *chi* angles were restricted to be in a range of −157° to −97° (*anti* conformation) for the canonical dG residues and of −10° to 90° (*syn* conformation) for the modified ones. The analysis was focalised on the 10 structures with the lowest CYANA target functions, that were then energy minimized (without angle constraints) using the CVFF forcefield and superimposed, giving average RMSD values of 2.39 ± 0.50 and 2.26 ± 0.45 for the backbone and all heavy atoms, respectively. As in the preceding cases, the resulting quadruplex structures of **M3** had a 4-fold symmetry with three hydrogen-bonding tetrads of almost co-planar guanine bases, that differ for Hoogsteen hydrogen bond length. In fact, the first two G-quartets of these structures showed H1–O6 and H21–N7 hydrogen bond lengths included in a range of 2.01–2.03 Å, that is typical of G-tetrad arrangements in canonical quadruplexes. The 8-Br-dG tetrad in the quadruplex structures formed by **M3** showed, instead, hydrogen bonds of length of 2.20–2.22 Å, suggesting that the presence of a bromine in the 8-position at this level does induce a distortion. In fact, all the structures determined for **M3** were affected by the presence of steric effects between bromine and the backbone of the adjacent strand (Fig. 4), and the base stacking is rather poor, accounting for the partial folding of this species in solution. In this case, the *chi* angles of the 8-Br-dG residues assumed values between −5° and 30°, falling perfectly in the *syn* range.

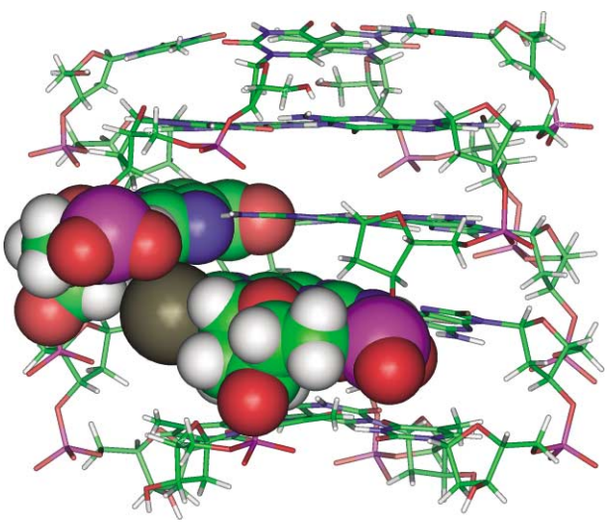

Fig. 4 Side view of average structure of the best 10 structures of the **M3** quadruplex. Heavy atoms are shown with different colors (carbons, green; nitrogens, blue; oxygens, red; hydrogens, white; bromine, dark brown); One 8-Br-dG residue and the dG residue of the adjacent strand are reported in CPK. As for the **M2** quadruplex, the steric effect between bromine and the 5′-phosphate group of guanosine of the adjacent strand is plainly observable.

CD spectroscopy of M1, M2 and M3

CD spectra for **M1**, **M2** and **M3** samples were acquired at 293 K. Surprisingly, the introduction of an 8-Br-dG residue in different positions of the same sequence 5′-d(TGGGT)-3′ provides very different CD spectra (Fig. 5). Particularly, the **M1** and **M3** samples showed unusual CD profiles, that differ widely from the spectra usually recorded for quadruplexes involving four parallel strands.[31] In fact, the CD spectrum of **M1** exhibited two positive bands, at 296 and 263 nm, and one negative

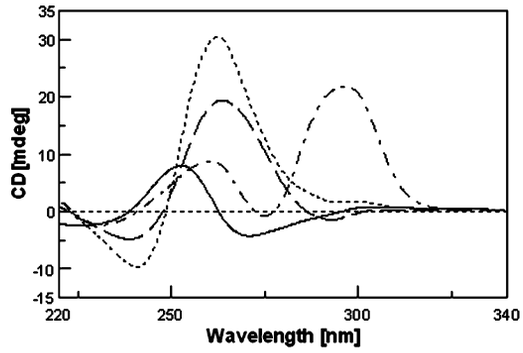

Fig. 5 CD spectra of $[d(TGGGT)]_4$ (— —), **M1** (- –), **M2** (- -) and **M3** (——).

band at 233 nm, whereas, the CD profile of **M3** was characterised by the presence of maximum and minimum Cotton effects at 256 nm and 275 nm, respectively. However, it should be noted that **M3** at 300 K exists as an equilibrium between a single strand and a quadruplex structure, and this might affect the aspect of its CD spectrum. Finally, the CD spectrum of **M2** was very similar to that of $[d(TGGGT)]_4$ and therefore characterised by maximum and minimum Cotton effects at 263 and 243 nm, respectively. These data suggest that 8-Br-dG residues do affect the structure of the quadruplexes and that, as expected, 8-Br-dG residues actually adopt a *syn* glycosidic conformation.

CD thermal denaturation experiments for M1, M2 and M3

In order to estimate the effects of the substitution of a canonical dG residue with an 8-Br-dG unit on the thermal stability of the quadruplexes adopted by **M1**, **M2** and **M3**, CD thermal denaturation experiments were performed. All the measurements were performed at a concentration of 5×10^{-5} M. Taking into account that the rates of quadruplex formation/dissociation are extremely slow, to avoid a kinetic influence on the collected data, we allowed thermodynamic equilibrium to be reached at any temperature as follows. The equilibrium melting curves for all the quadruplexes were obtained by collecting data in the range 5–65 °C using a temperature step of 5 °C and leaving the samples to equilibrate for a suitable time (see experimental section) after each temperature step before recording the CD. The CD signal at 263 nm was reported as function of temperature for all the studied quadruplexes. Then, the melting temperatures were derived by the inflection point of the sigmoidal curves obtained by fitting the experimental data (Fig. 6). This resulted in a T_m of 38.9 °C, 29.2 °C and 25.6 °C for the quadruplexes formed by **M1**, **M2** and the canonical quadruplex $[d(TGGGT)]_4$ respectively. It is not possible to estimate a melting temperature for the **M3** quadruplex because it begins to melt at a temperature that was not experimentally accessible (T_m < 15 C°). These data show that both quadru-

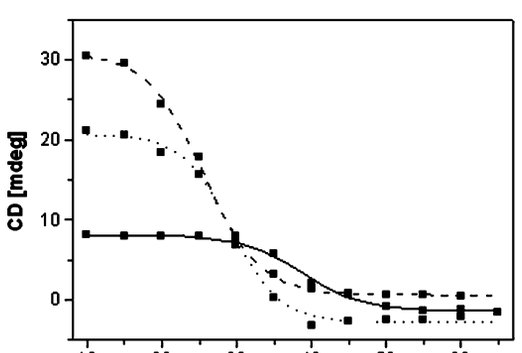

Fig. 6 CD thermal denaturation spectra of $[d(TGGGT)]_4$ (— —), **M1** (——), **M2** (. . . .).

plexes formed by **M1** and **M2** are thermally more stable than the unmodified counterpart, while the same substitution of the dG near the dT at the 3′ position, as for **M3**, results in a decrease in stability, signifying that the thermal stability depends strictly on the position of the modified base.

The results of these investigations are in general agreement with the data obtained from NMR, molecular mechanics and dynamics calculations. In fact, in the case of **M1**, the quadruplex structure generated is highly symmetric and without any distortion. The presence of the bromine in the C8 position of the dG at the 5′ edge of the fragment GGG seems to favour guanine base stacking with the adjacent G-tetrad (Fig. 1), resulting in the highest thermal stability recorded for this species. As concerning the quadruplex structure determined for **M2**, it is characterised by guanine residues to have an almost planar conformation with three well-defined G-tetrads. However, the steric effects between bromines and 5′-phosphate groups of adjacent strands (Fig. 2), and the only partial stacking between the five-membered rings of the 8-Br-dG residues and the five-membered rings of the underneath guanines (Fig. 3) may justify the lower thermal stability in comparison to that observed for the quadruplex formed by **M1**. On the other hand, the higher thermal stability of **M2** quadruplex (with respect to the unmodified quadruplex) could be explained by taking into account a further stacking between the six-membered rings of 8-Br-dG residues and the six-membered rings of the upper guanines (Fig. 3), and four additional H-bonds (H22 or H21/OP2) found in the final structures. The introduction of a bromine seems to have, on the contrary, serious effects on the quadruplex structure adopted by **M3**, that result in lower thermal stability and cause it to coexist with its single strand in solution at 300 K. The quadruplex structure determined in this case is affected by the presence of steric effects between bromine and the backbone of the adjacent strand. The base stacking is negligible and the Hoogsteen hydrogen bond length for the 8-Br-dG tetrad is wider than usual, probably because of perturbation due to the presence of the bulky substituent.

Conclusions

In this paper we report a combined NMR, molecular mechanics and dynamics calculations and CD spectroscopy characterization of three quadruplexes $[d(TG^{Br}GGT)]_4$, $[d(TGG^{Br}GT)]_4$ and $[d(TGGG^{Br}T)]_4$, where an 8-Br-dG residue was alternately introduced in the different positions of the sequence 5′-d(TGGGT)-3′.

We have found that all three modified oligomers, **M1**, **M2** and **M3**, form parallel stranded quadruplexes with all guanines, including 8-Br-dG residues, involved in hydrogen bonded tetrads. Interestingly, the introduction of an 8-Br-dG residue in different positions of the same sequence 5′-d(TGGGT)-3′ provides very different CD spectra (Fig. 5). The CD spectrum of **M2** shows the characteristic bands of parallel stranded quadruplexes and is comparable with that of $[d(TGGGT)]_4$, whereas the incorporation of an 8-Br-dG unit in the other positions of GGG tract (**M1** and **M3**), causes significant changes over the whole range of the CD spectra. Furthermore, different melting temperatures were also obtained. Particularly, **M1** and **M2** are respectively 13.3 and 3.6 °C more stable than the unmodified quadruplex, whereas it was not possible to measure the T_m for **M3**.

Finally, the structures reported here are, to the best of our knowledge, the first parallel quadruplexes possessing a 4-fold symmetry with all strands parallel to each other and containing one tetrad (formed by 8-Br-dGs) in a *syn* conformation, while the other two tetrads were still characterised by dGs possessing an *anti* glycosidic conformation. Numerous examples exist where nucleic acids (including quadruplex structures) have been selected as aptamers for proteins or small molecules.[37] Thus, the new structural features found in the three new structures reported could be used, in principle, for the creation of novel aptameric and catalytic nucleic acids in order to provide novel structural motifs for ligand-binding pockets with diverse molecular recognition capabilities that would not be present using native RNA/DNA sequences.

Experimental

The oligonucleotides **M1**, **M2** and **M3** were synthesized on a Millipore Cyclon Plus DNA synthesizer, using solid phase β-cyanoethyl phosphoramidite chemistry at 15 μmol scale. The oligomers were detached from the support and deprotected by treatment with conc. aqueous ammonia at 55 °C for 12 h. The combined filtrates and washings were concentrated under reduced pressure, redissolved in H_2O and analysed and purified by HPLC on a Nucleogel SAX column (Macherey-Nagel, 1000–8/46); using buffer A: 20 mM KH_2PO_4 aq. solution, pH 7.0, containing 20% (v/v) CH_3CN; buffer B: 1 M KCl, 20 mM KH_2PO_4 aq. solution, pH 7.0, containing 20% (v/v) CH_3CN; a linear gradient from 0 to 100% B in 30 min and flow rate of 1 mL min^{-1} were used. The isolated oligomers have the following retention times: **M1** = 8.8 min (as single strand), 18.5 min (as quadruplex); **M2** = 8.5 min (as single strand), 17.6 min (as quadruplex); **M3** = 8.6 min (as single strand), 16.2 min (as quadruplex). The different fractions of the same oligomer were collected and successively desalted by Sep-Pak cartridges (C18). The isolated oligomers were more than 98% pure (NMR).

Nuclear magnetic resonance

NMR samples were prepared at a concentration of approximately 1 mM, in 0.5 ml (H_2O/D_2O 9 : 1) buffer solution having 10 mM KH_2PO_4, 70 mM KCl, 0.2 mM EDTA, pH 7.0. For D_2O experiments, the H_2O was replaced with D_2O by drying down the sample, lyophilization and redissolution in D_2O alone. NMR spectra were recorded with a Bruker AMX 500 spectrometer. 1D proton spectra of samples in H_2O were recorded using pulsed-field gradient WATERGATE[32] for H_2O suppression. Phase sensitive NOESY spectra[38] were recorded with mixing times of 100 and 200 ms (T = 300 K). Pulsed-field gradient WATERGATE was used for NOESY spectra in H_2O. TOCSY spectra[39] with mixing times of 120 ms were recorded with D_2O solutions. NOESY and TOCSY were recorded using TPPI[40] procedure for quadrature detection. In all 2D experiments the time domain data consisted of 2048 complex points in t_2 and 400–512 fids in t_1 dimension. The relaxation delay was kept at 1.2 s for all experiments. The NMR data were processed on a SGI Octane workstation using FELIX 98 software (Byosym, San Diego, CA).

Structural calculations

The structure calculations were performed with the CYANA program[36] starting from 300 random conformations. Upper limit distance constraints for both exchangeable and non-exchangeable hydrogens were classified according to their intensity in the NOESY spectra (mt = 100 ms) with the CALIBA tool of the CYANA program.[36] 256, 252 and 340 upper distance restraints were calculated for **M1**, **M2** and **M3**, respectively, and reduced to 112, 100 and 144 after removal of irrelevant restraints. Pseudo-atoms were introduced where needed. Hydrogen bond constraints (16 upper and 16 lower limit constraints/G-tetrad) were used: upper and lower distance limits of 2.0 Å and 1.7 Å for hydrogen–acceptor distance, and 3.0 Å and 2.7 Å for donor–acceptor distance, respectively. These constraints for H-bonds did not lead to an increase in residual constraints violation. Backbone torsion angles were restricted to be in a range of ±20° of the helical values of natural quadruplexes.[7] Glycosidic torsion angles for all unmodified guanines were kept in a range of −157° to −137° (*anti* conformation), whereas a range of −10° to 90° (*syn* conformation) was used for

8-Br-dG residues. The input for final CYANA structure calculations also included constraints to close the sugar rings (C4′–O4′: 1.41 Å, C4′–C1′: 2.40 Å, C5′–C4′: 2.39 Å, H4′–O4′: 2.12 Å). The dynamics run for 35000 steps (highsteps = 7000; minsteps = 7000). The 10 structures with the lowest CYANA target functions were subjected to energy minimization (with no angle constraint) by conjugate gradient methods as implemented in the DISCOVER program (Molecular Simulations, San Diego, CA, USA), using CVFF force field. During energy minimization, interproton distances and H-bond constraints involving G-tetrads were used with a force constant of 20 and 100 kcal mol^{-1} $Å^{-2}$, respectively. Illustrations of structures were generated with INSIGHTII program, version ′98 (Biosym Technologies Inc.). All the calculations were performed on an SGI Octane workstation.

Molecular modelling

Models of the quadruplex structures adopted by **M1**, **M2** and **M3** were performed with the CYANA program starting from 300 random conformations as described in the "structure calculation" section. The G, T and 8-Br-dG nucleotides were kept in *anti* glycosidic conformation. The three models with the lowest CYANA target function were then subjected to energy minimization by conjugate gradient methods as implemented in the DISCOVER program (Molecular Simulations, San Diego, CA, USA), using CVFF force field. During energy minimization, interproton distances and H-bond constraints involving G-tetrads were used with a force constant of 20 and 100 kcal mol^{-1} $Å^{-2}$, respectively. Illustrations of models were generated with INSIGHTII program, version ′98 (Biosym Technologies Inc.).

Circular dichroism

CD samples were prepared at a concentration of 10^{-5} M, by using a buffer solution having 10 mM KH_2PO_4, 70 mM KCl, 0.2 mM EDTA, pH 7.0. CD spectra of **M1**, **M2** and **M3** were registered on a Jasco 715 circular dichroism spectrophotometer in the same buffer used for NMR experiments at 20 °C in a 0.1 cm pathlength cuvette. The wavelength was varied from 220 to 340 nm at 5 nm min^{-1}, and the spectra recorded with a response of 16 s, at 2.0 nm bandwidth and normalized by subtraction of the background scan with buffer. The temperature was kept constant at 5 °C with a thermoelectrically controlled cell holder (JASCO PTC-348).

CD melting experiments

CD samples were prepared as described in the "circular dichroism" section. The equilibrium melting curves for all the quadruplexes were obtained by collecting data in the range 5–65 °C using a temperature step of 5 °C. The samples were incubated at each temperature to achieve the equilibrium before recording the CD. The reaching of equilibrium at each temperature was guaranteed by the achievement of a superimposable CD spectra on changing time. Up to 30 °C the equilibrium was reached after 48 hours, whereas, above this temperature, the equilibrium was achieved in a progressively shorter time. At 65 °C the equilibrium was reached in 16 hours. The melting curves were obtained reporting CD signal at 263 nm as a function of temperature. The melting temperatures were evaluated using the Boltzman fit of the Origin program. The error on the inflection point is <1%. The CD data were recorded in the same buffer used for NMR experiments in a 0.1 cm pathlength cuvette.

Acknowledgements

This work is supported by Italian M. U. R. S. T. (P. R. I. N. 2001 and 2002) and Regione Campania (L.41). The authors are grateful to "Centro Ricerche Interdipartimentale di Analisi Strumentale", C. R. I. A. S., for supplying NMR facilities. Anna Scarinzi, Ileana Cozzolino and Bruno Pagano are acknowledged for their kind collaboration.

References

1 E. Henderson, C. C. Hardin, S. K. Walk, I. Tinoco and E. H. Blackburn, Jr., *Cell*, 1987, **51**, 899–908.
2 R. F. Macaya, P. Schultze, F. W. Smith, J. A. Roe and J. Feigon, *Proc. Natl. Acad. Sci. U. S. A.*, 1993, **334**, 3745–3749.
3 Y. Wang and D. J. Patel, *J. Mol. Biol.*, 1995, **251**, 76–94.
4 P. Schultze, W. S. Flint and J. Feigon, *Structure*, 1994, **2**, 221–233.
5 F. W. Smith and J. Feigon, *Nature*, 1992, **356**, 164–168.
6 F. Aboul-ela, A. I. H. Murchie, D. G. Norman and D. M. J. Lilley, *J. Mol. Biol.*, 1994, **243**, 458–471.
7 P. K. Patel, A. S. R. Koti and R. V. Hosur, *Nucleic Acids Res.*, 1999, **27**, 3836.
8 D. Sen and W. Gilbert, *Nature*, 1988, **334**, 364–366.
9 D. Sen and W. Gilbert, *Nature*, 1990, **334**, 410–414.
10 D. Sen and W. Gilbert, *Biochemistry*, 1992, **31**, 65–70.
11 (*a*) G. Laughlan, A. I. H. Murchie, D. G. Norman, M. H. Moore, P. C. E. Moody, D. M. J. Lilley and B. Luisi, *Science*, 1994, **265**, 520–524; (*b*) K. Phillips, Z. A. Dauter, I. H. Murchie, D. M. J. Lilley and B. Luisi, *J. Mol. Biol.*, 1997, **273**, 171–182.
12 Y. Wang and D. J. Patel, *Structure*, 1993, **1**, 263–282.
13 P. Catasti, X. Chen, R. K. Moyzis, E. M. Bradbury and G. Gupta, *J. Mol. Biol.*, 1996, **264**, 534–545.
14 C. Kang, X. Zhang, R. Ratliff, R. Moyzis and A. Rich, *Nature*, 1992, **356**, 126–131.
15 P. Schultze, R. F. Macaya and J. Feigon, *J. Mol. Biol.*, 1994, **235**, 1532–1547.
16 E. R. Henderson and E. H. Blackburn, *Mol. Cell. Biol.*, 1989, **9**, 345–348.
17 E. H. Blackburn, *Nature (London)*, 1991, **350**, 569–573.
18 T. Nikaido, Y. Yamawaki-Kataoka and T. Honjo, *J. Biol. Chem.*, 1982, **257**, 7322–7329.
19 J. Jeffreys, V. Wilson and S. L. Thein, *Nature (London)*, 1985, **314**, 67–73.
20 D. A. Collier, J. A. Griffin and R. D. Wells, *J. Biol. Chem.*, 1988, **263**, 7397–7405.
21 N. D. Hastie and R. C. Allshire, *Trends Genet.*, 1989, **5**, 326–331.
22 S. A. Akman, R. G. Lingeman, J. H. Doroshow and S. S. Smith, *Biochemistry*, 1991, **30**, 8648–8653.
23 J. M. Nickol and G. Felsenfeld, *Cell*, 1983, **35**, 467–477.
24 T. Simonsson, P. Pecinka and M. Kubista, *Nucleic Acids Res.*, 1998, **26**, 1167–1172.
25 M. C. Hammond-Kosack, M. W. Kilpatrick and K. Docherty, *J. Mol. Endocrinol.*, 1992, **9**, 221–225.
26 W. Deng, A. Parbhu-Patel, D. J. Meyer and D. A. Baker, *Biochem. J.*, 2003, **374**, 559–565 and references cited therein.
27 (*a*) M. Ioele, R. Bazzanini, C. Chatgilialoglu and Q. G. Mulazzani, *J. Am. Chem. Soc.*, 2000, **122**, 1900–1907; (*b*) T. Carell, C. Behrens and J. Gierlich, *Org. Biomol. Chem.*, 2003, **1**, 2221–2228.
28 D. J. Proctor, E. Kierzek, R. Kierzek and E. P. C. Bevilacqua, *J. Am. Chem. Soc.*, 2003, **125**, 2390–2391.
29 E. Dias, J. L. Battiste and J. R. Williamson, *J. Am. Chem. Soc.*, 1994, **116**, 4479–4480.
30 (*a*) S. Uesugi and M. Ikehara, *J. Am. Chem. Soc.*, 1977, **99**, 3250; (*b*) F. Jordan and H. Niv, *Biochim. Biophys. Acta*, 1977, **476**, 265; (*c*) S. Uesugi, M. Ohkubo, H. Urata, M. Ikeara, Y. Kobayashi and Y. Kyogoku, *J. Am. Chem. Soc.*, 1984, **106**, 3675.
31 J. Renzhe, L. B. L. Gaffney, C. Wang, R. A. Jones and K. J. Breslauer, *Proc. Natl. Acad. Sci. U. S. A.*, 1992, **89**, 8832–8836.
32 M. Piotto, V. Saudek and V. J. Sklenar, *J. Biomol. NMR*, 1992, **2**, 661–665.
33 K. Y. Wang, S. McCurdy, R. G. Shea, S. Swaminathan and P. H. Bolton, *Biochemistry*, 1993, **32**, 1899–1904.
34 P. K. Patel, N. S. Bhavesh and R. V. Hosur, *Biochem. Biophys. Res. Commun.*, 2000, **270**, 967–971.
35 P. K. Patel and R. V. Hosur, *Nucleic Acids Res.*, 1999, **27**, 2457–2464.
36 P. Guntert, C. Mumenthaler and K. Wuthrich, *J. Mol. Biol.*, 1997, **273**, 283–298.
37 S. E. Osborne, I. Matsumura and A. D. Ellington, *Curr. Opin. Chem. Biol.*, 1997, **1**, 5–9.
38 J. Jeener, B. H. Meier, P. Bachmann and R. R. Ernst, *J. Chem. Phys.*, 1979, **71**, 4546–4553.
39 L. Braunschweiler and R. R. Ernst, *J. Magn. Reson.*, 1983, **53**, 521–528.
40 D. Marion and K. Wuthrich, *Biochem. Biophys. Res. Commun.*, 1983, **113**, 967–874.